Fragmentation of diffusion zone in high-temperature oxidation of copper

V.V. Prisedsky*, V.M. Vinogradov

Faculty of Chemistry and Technology, Department of General Chemistry, Donetsk National Technical University, 58 Artema, Donetsk 83000, Ukraine

Abstract

Using thermogravimetry, microscopy and X-ray diffraction, high-temperature (600–900 °C) oxidation of copper wires and plates has been studied. An abrupt decrease in reaction rate after complete consumption of metal phase but long before reaching equilibrium has been observed. This phenomenon is connected to an irregular character of the development of the reaction diffusion zone. In contrast to the usually applied layer model, initially formed oxide layers separate into numerous aggregates of Cu_2O crystals chaotically scattered throughout the zone between thinner layers of CuO grains. Such fragmentation of the diffusion zone is induced by macro- and microcracks formed in copper scale under influence of mechanical stresses at metal-oxide phase boundary due to the difference in molar volume between copper and its oxides. The pattern of cracks provides channels of fast diffusion and maintains the reaction rate at high level but only until the source of crack formation remains in action.
© 2004 Elsevier Inc. All rights reserved.

Keywords: Copper; Copper oxides; Oxidation; Kinetics; Reaction diffusion; Diffusion zone; Structure of diffusion zone

1. Introduction

A very special place occupied by copper in the history of human civilization seems to remind of itself again in the unique role of cuprates among high-temperature superconductors and other advanced materials intensively studied during the last decades. This supports the interest to many aspects of copper physical and chemical behavior and, in particular, to the properties of copper oxides and their formation.

The phase equilibria and nonstoichiometry of oxides in the system Cu–O have been studied, starting with classical works of the first half of the 20th century, quite completely and reviewed in many literature sources, e.g., [1–4]. The data of different authors on the kinetics of high-temperature oxidation of metallic copper to oxide Cu_2O agree with each other as well as with the measurements of electrical conductivity and isotope diffusion [1,2,4–7]. At the same time, the details of deeper copper oxidation to CuO are much less lucid. In fact, there are no reports on kinetic studies in the course of complete copper oxidation to single-phased CuO as an equilibrium product. Valenci (as cited in [4,6]) noticed that the copper scale formed on metallic surface in air up to 1000 °C contains both CuO and Cu_2O layers in ratio that depends on the temperature of oxidation. It has been reported also that copper scale contains both CuO and Cu_2O not only in the course of reaction but also after complete oxidation of metallic phase [5,6]. This observation shows that equilibrium state was not reached in these studies otherwise it contradicts to both phase rule and $p(O_2)$–T phase diagram [1] according to which the equilibrium phase under stated conditions is CuO. In spite of these facts, the reported data on the parabolic rate constants of copper scale formation in air are in fair agreement between each other [1,2,5,6].

*Corresponding author.

E-mail address: prisedsky@feht.dgtu.donetsk.ua (V.V. Prisedsky).

The aim of this work is the study of oxidation kinetics and also composition, structure and development of reaction diffusion zone in the course of copper oxidation in air in temperature interval 600–900 °C.

2. Experimental

The specimens of electro-technical copper 99.99% pure in the form of wires 0.30 and 1.7 mm in diameter and also plates 0.10 and 0.50 mm thick have been used in the study.

The equilibria and kinetics of copper oxidation were studied gravimetrically in the experimental setup shown schematically in Fig. 1. Continuous measurement of the specimen mass (± 0.1 mg) was conducted by an electronic balance (VLA-200, Novosibirsk) connected to a recording potentiometer. The specimen was suspended with a Pt wire inside a vertical quartz tube in an electrical furnace with NiCr heaters [8]. The temperature near the specimen was measured with a PtRh–Pt thermocouple and regulated with the accuracy ± 0.2 °C using another PtRh–Pt thermocouple placed close to the heaters and connected to a thyristor scheme. Times to achieve fixed temperature for isothermal treatments (during 6–100 h) were less than 45 min. The flux of flowing gas (air in most cases) used to control a specified oxygen partial pressure $p(O_2)$ was adjusted so that the specimen buoyancy was less than 0.05 mg. The value of $p(O_2)$ was monitored with an oxygen concentration cell using yttria-stabilized zirconia (YSZ) as an oxygen conducting electrolyte.
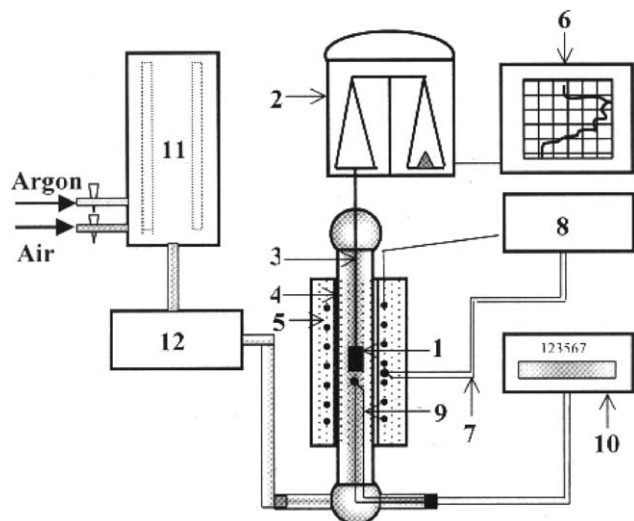
Fig. 1. The apparatus for thermogravimetry: (1) specimen; (2) electronic balance VLE-200; (3) Pt wire suspension; (4) quartz tube reactor; (5) furnace; (6) recording potentiometer KSP-4; (7) regulating PtRh–Pt thermocouple; (8) thyristor regulator VRT-3; (9) control PtRh–Pt thermocouple; (10) digital millivoltmeter V7-34A; (11) gas mixer; and (12) $p(O_2)$ electrochemical meter.

Optical microscopy (Biolam C-11 and MIM-7 microscopes) was used to study the structure of the reaction zone on polished cross-sections of specimens oxidized at a given temperature for a predetermined time. For that purpose oxidized wires or plates were put into epoxy resin and, after its solidification, lapped and polished with diamond paste. Micrographs were taken with a mirror photocamera (Zenith, Moscow) mounted by means of an adjusting ring to the microscope.

A DRON-3 diffractometer operating on Fe$K\alpha$ radiation was used for X-ray diffraction (XRD) analysis.

3. Results and their discussion

3.1. Retardation of oxidation kinetics

The results of gravimetric study of copper oxidation under isothermal conditions at 600, 700, 800 and 900 °C in air are presented in Fig. 2 as dependences of the overall oxygen content in the specimen, expressed as x in CuO_x, on time. In all experimental runs, an abrupt decrease in reaction rate is observed at values of x somewhat higher than 0.5. For example, the average oxygen content in the specimen of copper wire 1.7 mm in diameter reaches $x = 0.50$ after 38 h of oxidation at 900 °C (Fig. 2d). Then, during the next 8 h, it increases to $x = 0.54$, and only to $x = 0.56$ in the following 50 h of treatment at 900 °C. The slope of the kinetic curve decreases more than an order of magnitude as x changes from 0.52 to 0.55. In this case, even increasing temperature does not help to reestablish a higher oxidation rate: further heating of this specimen at 970 °C for another 32 h resulted only in a very small increase, $\Delta x < 0.01$, in overall oxygen content.

As seen in Fig. 2, an abrupt decrease in oxidation rate has been observed on all specimens, both wires and plates, thicker and thinner, and at all temperatures provided that the time of reaction was long enough to oxidize a specimen to $x \geqslant 0.5$. The overall specimen composition at the onset of the reaction slow-down is found to lie between $CuO_{0.52}$ and $CuO_{0.56}$ with larger x values usually being found for higher reaction rates on thinner specimens. An unambiguous dependence of this composition on temperature of oxidation has not been found.

Microscopic observations and powder XRD investigations reveal no remains of metallic copper in specimens just after the slow-down of oxidation. At this stage, the oxidized specimen presents all of itself as breakable copper scale composed of a two-phase mixture of copper oxides Cu_2O and CuO with predominance of Cu_2O as indicated by XRD analysis (Fig. 3c). Therefore, the abrupt decrease of the reaction rate occurs at the moment when the metallic phase is consumed in the reaction and only in this sense it
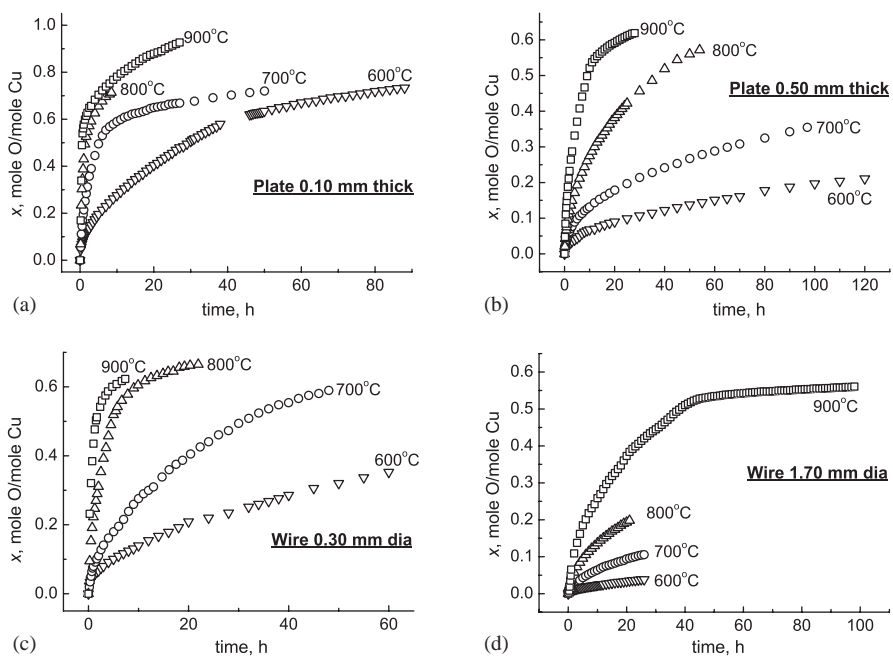
Fig. 2. Kinetics of oxidation of various copper specimens in air. Index x expresses the overall oxygen molar content in an oxidized specimen CuO_x.
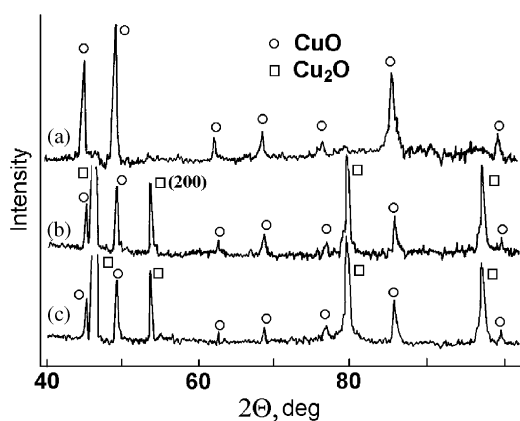
Fig. 3. X-ray powder diffraction patterns of copper samples oxidized in air: (a) separated scale, 600 °C, 2 h; (b) separated scale, 700 °C, 4 h; and (c) oxidized plate 0.50 mm, 900 °C, 12 h.

corresponds to complete oxidation of copper. The oxidation process at this point is still far from its equilibrium ($x \approx 1.00$) as the whole temperature interval studied lies within the CuO stability region in the phase diagram [1,2,10]. However, further oxidation proceeds so slow that the two-phased copper scale could be easily taken for its final product. The transfer of the same particles, copper and oxygen atoms or ions, free electrons or electron holes, through the same oxide phases is required to maintain oxidation both in the presence of metallic phase and after its complete consumption. Taking that into account, a sharp decrease in oxidation rate at that moment deserves further consideration.

The average composition of copper scale formed just after the oxidation slow-down is found to lie in the interval $x = 0.55{-}0.60$ at all studied temperatures. It means that 90–80 mol% of copper, respectively, is present in the form of cuprite Cu_2O in the scale at this moment of reaction, whereas the molar fraction of the ultimate product of oxidation, tenorite CuO, is only 10–20 mol%.

Valensi [4,6] used a two-layer model for describing the structure of copper scale in which each layer, external one of CuO and internal one of Cu_2O, retained its own value of the parabolic growth rate constant. He calculated the ratio of thicknesses of two oxide layers and showed that it was steady in the course of scale growth but depended on temperature of oxidation. Paidassi [9] reported lower values for relative thickness of CuO layer and found that CuO content in copper scale increased with time of oxidation. Even lower estimation for the thickness of CuO layer was obtained by Hauffe [6]. Our data on the composition of copper scale after the reaction slow-down agree well with Valenci's calculation for growing double-layer scale at 900 °C, but are closer to Paidassi's results at lower temperatures. More important distinction concerns the observation of the abrupt decrease in reaction rate. In earlier works [2,4–6,9] the kinetics of deep copper oxidation were not reported.

In spite of high stability of two-phased copper scale after the oxidation slow-down, the samples of such scale may be easily reoxidized (e.g., 2 h at 750 °C on Pt plate) to equilibrium oxide CuO after their grinding into a fine powder (in an agate mortar, under ethanol). This fact

indicates that the reaction slow-down is an attribute of oxidation to rather thick scale layers on compact copper specimens. It is directly related to peculiar features of the structure of such layers.

3.2. Oxidation in ambients with diverse oxygen pressure

Fig. 4 presents $x–t$ kinetic curves of copper oxidation at 900 °C in three gaseous ambients with various partial oxygen pressures: (a) air, $p(O_2) = 0.21$ atm; (b) mixture of argon with air with $p(O_2) = 10^{-3}$ atm; (c) argon with residual $p(O_2) = 2 \times 10^{-5}$ atm. The first two of these pressures correspond to the CuO stability region in the Cu–O phase diagram, whereas the third one is lower than the dissociation pressure of CuO at this temperature and lies in the stability region of Cu_2O [1,10]. As confirmed by XRD and seen from the configuration of the kinetic curve, oxidation under the lowest $p(O_2)$ ends in formation of single-phased cuprite Cu_2O. It is the equilibrium phase under the specified thermodynamic conditions, although reaching exact equilibrium oxygen content within the narrow homogeneity region of Cu_2O remains beyond the scope of this consideration. In contrast, oxidation under two higher $p(O_2)$ yields a two-phased product which is yet far from equilibrium in the sense of both phase state and overall composition ($x < 1$). The abrupt decrease of the reaction rate is observed in these two cases, but no signs of the reaction retardation are visible if only single-phased Cu_2O is produced.

In spite of this difference, all three kinetic curves lie very close to each other at $x < 0.5$. Only slight reduction in oxidation rate with lowering oxygen pressure may be noticed.

This fact leads to the following two conclusions. First, the chemical potential of oxygen in gas ambient does not affect the rate of reaction. Such stages of oxidation as oxygen transfer to the scale surface (including such transfer in tiny pores likely to occur in the scale) or oxygen adsorption do not play the role of the limiting stage. The overall rate of the reaction is determined by diffusion in solid phases. Second, taking into account that Cu_2O is present as a reaction product in all three experiments, the diffusion through cuprite phase may be considered as a rate determining stage for copper oxidation.

3.3. Parabolic scale growth and rate constants

In the interval $0 < x < 0.5$, kinetic curves are linear in quadratic coordinates (Fig. 5) demonstrating that the kinetics of oxidation before the reaction slow-down follows the parabolic law:

$$(\Delta m/S)^2 = k\tau$$

where Δm is the change in the specimen's mass due to oxygen uptake, g; S the specimen's surface, cm^2; and τ the time for that change to occur, h. This fact indicates a diffusion control of the reaction rate. Systematic deviation of experimental points from the linear part of the $(\Delta m/S)^2$ against τ graph were used as a more appropriate means to decide if an unexpected decrease in reaction rate occurs and to determine precisely its onset.

The calculated values of parabolic rate constant k are presented in Table 1. Their temperature dependence obeys the Arrhenius equation (Fig. 6). The Arrhenius parameters for experimental sets on each specimen are also given in Table 1.

A spread of the data between thinner and thicker specimens may be connected to a larger inaccuracy introduced by a nonisothermal period of heating a specimen to a specified temperature in the former case. Taking that into account and excluding the data for thinner specimens from statistical population in calculating the parameters, the following equation for the temperature dependence of oxidation rate has been obtained:

$$k = (68.0 \pm 1.2) \exp\{-(134.700 \pm 1.700)/RT\}.$$

The found value of activation energy, $E_A = 134.7$ kJ/mol, corresponds to that reported for reaction $2Cu + \frac{1}{2}O_2 = Cu_2O$ [1,4].

Comparison of rate constants determined here with the values found by different authors and reviewed in [4,5,13] (Fig. 6) shows their agreement. This fact implies, in particular, that in cited previous works exactly the same stages of reaction, i.e., before the reaction slow-down, were studied.

It is noteworthy, that a more detailed examination of the kinetic curves shows that reaction rate does not obey strictly the parabolic law at the very beginning of oxidation. Linear parts on the plot of x vs. t are visible at the initial stage ($x < 0.07$) of oxidation at
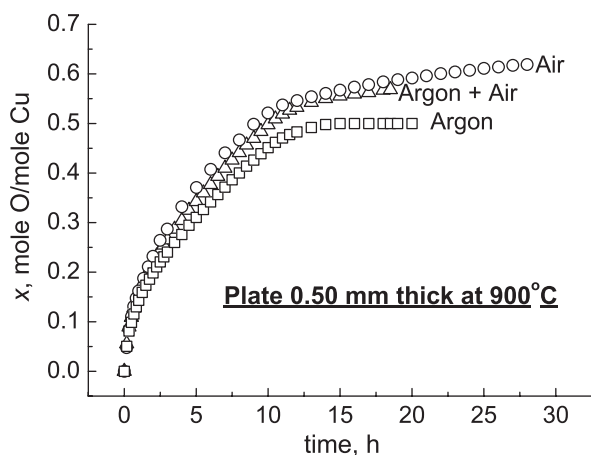
Fig. 4. Kinetics of copper oxidation under various oxygen pressures at 900 °C.
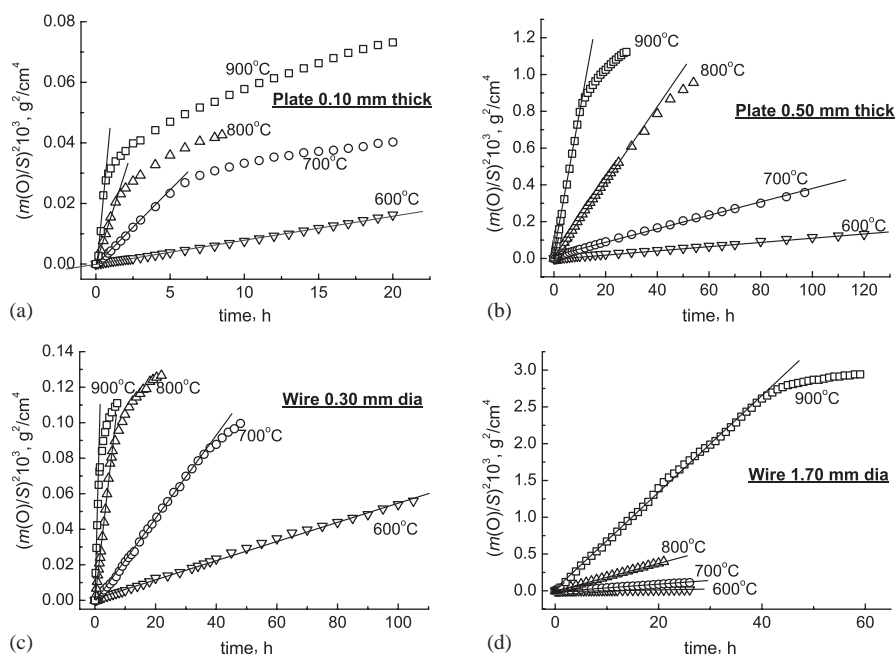
Fig. 5. Linearity of initial parts of kinetic curves in quadratic coordinates. Deviation of experimental points from the linear part of the kinetic plot shows exactly when the oxidation slow-down starts.

Table 1
Parabolic rate constants k and parameters of the Arrhenius plot for copper oxidation in air

Specimen	$k \times 10^6$, g^2/(cm^4 h), at temperature (°C)				Parameters of the Arrhenius plot	
	600	700	800	900	Frequency factor A	Activation energy E_A (kJ/mol)
Wire 1.70 mm dia.	0.570 ± 0.005	4.50 ± 0.03	19.1 ± 0.05	66.4 ± 0.4	67.0 ± 1.5	134.4 ± 3.3
Wire 0.30 mm dia.	0.562 ± 0.006	3.56 ± 0.02	16.2 ± 0.02	50.6 ± 1.4	27.1 ± 1.2	128.3 ± 1.8
Plate 0.5 mm thick	0.610 ± 0.007	3.76 ± 0.04	18.3 ± 0.02	70.8 ± 0.3	69.2 ± 1.3	134.8 ± 2.2
Plate 0.1 mm thick	0.634 ± 0.009	4.66 ± 0.006	16.7 ± 0.02	67.2 ± 3.1	40.1 ± 1.7	130.4 ± 4.5
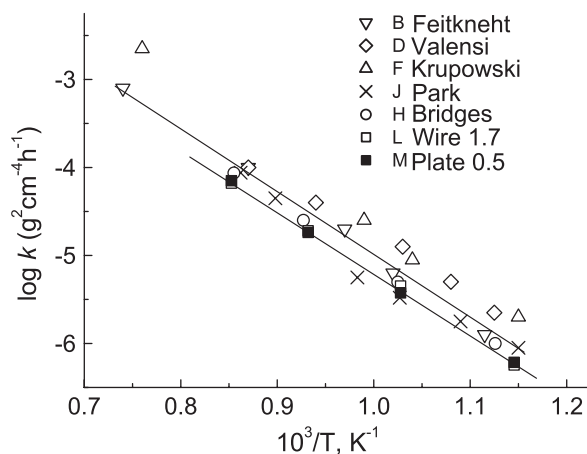
Fig. 6. Comparison of our (L,M) and literature (B,D,F [4,5] and J,H [13]) data on the temperature dependence of the parabolic rate constant for copper oxidation.

600 °C (Fig. 7), implying a possibility of the rate control by oxygen transport to the surface of a specimen.

3.4. Microscopic structure of diffusion zone

Microscopic photographs of polished cross-sections and cleaved fragments of samples taken at different stages of specimen oxidation are presented in Fig. 8. In all micrographs, the boundary between scale and metal looks quite regular geometrically, so that at each moment the thickness of scale layer does not vary much along the surface of the specimen.

At the very first moments of oxidation (at $T < 800$ °C) numerous CuO whiskers appear on the surface of copper specimen (Fig. 8a). Then these black needle-like crystals thicken into a porous layer of lustreless black phase similar to soot in consistency. This layer is growing rapidly and in 1–2 h at 700 °C reaches up to
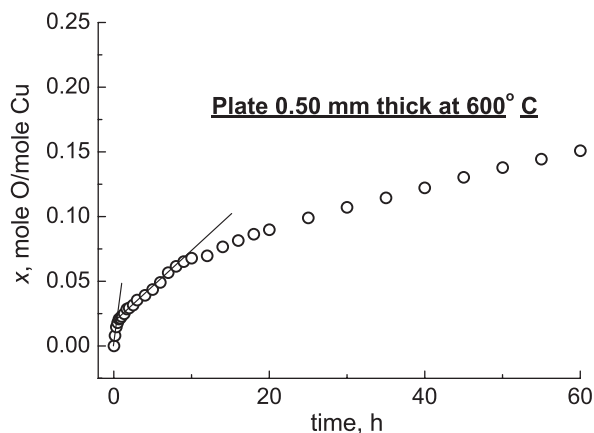
Fig. 7. Linear sections in the initial part of $x-t$ kinetic curve at 600 °C.

50–70 μm in thickness. The scale is not yet strongly bond to copper surface at this moment and easily separates from it, e.g., during rapid cooling due to the difference in thermal expansion between metallic and oxide phases. The XRD pattern from such detached scale samples shows the reflections only from CuO phase (Fig. 3a). This scale is practically single-phased and no cuprite phase Cu_2O is observed.

In further oxidation, increasing density of needle-like crystals leads to their recrystallization into grains of almost equiaxial habitus. The recrystallized grains look grayish and bright under microscope due to strong light reflections at their well-formed facets. In some time, e.g., 2–3 h at 700 °C, on outer surface of the specimen a continuous dense layer of recrystallized grains of up to 20 μm thick is formed over lustreless black phase of fine-grained tenorite phase CuO (Fig. 8b).

After that, well-edged crystal grains of bright-red phase Cu_2O appear at the phase boundary with metal and then quickly grow. On the micrograph of a fractured fragment of a specimen at this stage of oxidation (Fig. 8c), the layer of red Cu_2O grains (4) is seen above the surface of metallic copper (1), lighter in color, and under the grayish layer of recrystallized CuO (3). Numerous pits of reaction etching are visible on the surface of copper separated from scale indicating that copper ion transfer in reaction is orientation dependent in the crystal-grain range. The cuprite layer in Fig. 8c is now thicker than that of tenorite, whereas grains of Cu_2O were practically invisible in the scale before. The cuprite layer has grown at the expense of the earlier formed tenorite. From repeated microscopic observations, the ratio of CuO to Cu_2O layer thickness shifts at this stage to about 1:10.

The XRD pattern from the scale (separated from metal substrate) at this stage of oxidation shows a two-phased mixture of CuO and Cu_2O in which cuprite phase dominates (Fig. 3b). During a long period from that moment to the oxidation slow-down, the scales display quite similar XRD patterns (compare Figs. 3b and c) corroborating the fact that overall Cu_2O/CuO composition ratio does not change much in the scale for all that time.

The next stage of oxidation brings even more profound rearrangements in the diffusion zone. As seen in Fig. 8d, the layer of copper scale (700 °C, 20 h) now breaks into many Cu_2O crystal aggregates separated by thinner layers of black or grayish CuO crystals. Such fragmentation of the reaction diffusion zone comprises all the volume of copper scale with the exception of thin outer layer (3) of already recrystallized CuO grains and inner layer (4) consisting of only red Cu_2O crystals (Fig. 8d).

The fragmentation of the diffusion zone remains a predominant feature in the following stages of copper oxidation. Fig. 8e shows the spread of fragmentation throughout the cross-section of a wire after complete oxidation of metallic phase. Hollows seen in the center of the specimen indicate outward direction of predominant mass transfer in the reaction.

For comparison, the micrograph of a single-phased cuprite layer obtained by copper oxidation at 900 °C in argon (residual $p(O_2) = 10^{-5}$ atm) is presented in Fig. 8f. This is in apparent contrast with complicated entangled patterns in fragmented two-phased copper scale.

In the micrograph of oxidized copper foil (Fig. 8(g), a narrow strip of single-phased cuprite is seen in the center of the specimen. It has not undergone fragmentation. Such strips are often observed in the central parts of oxidized specimens just after the reaction slow-down. In the fragmented parts of scale, more often the black phase is seen under microscope indicating that it is spread on the surfaces of easy cracking, which are readily exposed when polishing the sample.

Increasing temperature of oxidation intensifies the recrystallization of tenorite crystals in greater extent than that of cuprite. In Fig. 8h textured plate-like CuO grains densely packed into stacks of up to 50 μm thick are seen surrounding red Cu_2O grains about the same in measurements as those at lower temperatures. Increasing density of CuO grains contributes into slowing copper scale oxidation to equilibrium single-phased CuO.

3.5. Discussion of the observed structure of the diffusion zone and its development

The scheme summarizing the development of the diffusion zone based on microscopic observations is presented in Fig. 9.

At the early stage of oxidation, CuO whiskers (Fig. 9a) and their aggregates thickened into a layer of fine-grained tenorite (Fig. 9b) behave as quite permeable to gas ambient providing a possibility of fast oxygen transfer through vast open pores in the growing oxide
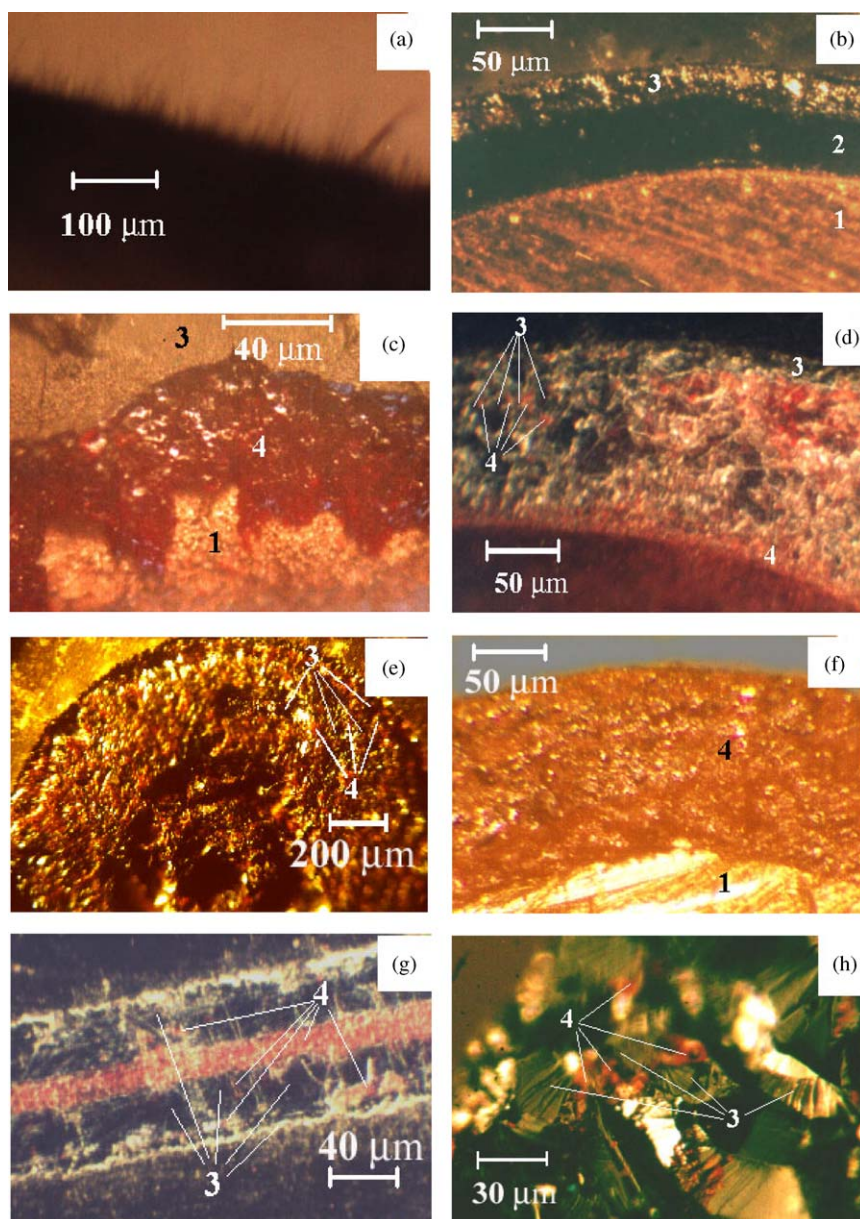
Fig. 8. Micrographs of reaction diffusion zone: (a) CuO whiskers (600 °C, 2 h); (b) gray lustrous layer of recrystallized CuO grains (3) over the black layer of lusterless fine-grained CuO (2) (700 °C, 2 h); (c) a fractured fragment of two-layered copper scale: bright red crystals of Cu_2O (4) lie over Cu surface (1) and under thinner gray layer of CuO (3) (700 °C, 4 h); (d) a fragmented layer of copper scale: small aggregates of Cu_2O crystals are separated by thin black or gray layers of CuO (700 °C, 20 h); (e) cross-section of a wire specimen after complete oxidation of metallic phase (900 °C, 48 h); (f) single-phased Cu_2O layer obtained by copper oxidation at 900 °C in argon; (g) cross-section of oxidized copper foil after the reaction slow-down (800 °C, 2 h); (h) dense stacks of recrystallized plate-like grains of CuO (3) surrounding grains of cuprite Cu_2O (4) (975 °C, 32 h). Phases: (1) Cu; (2) CuO fine-grained; (3) CuO recrystallized; and (4) Cu_2O.

layer. This is in agreement with observed linear sections in the initial part of x vs. t plot in Fig. 7. The rate of oxidation at this stage is not yet controlled by diffusion in solid phase.

The diffusion control of the reaction rate is established after a dense layer of recrystallized tenorite grains is formed on the outer surface of the growing copper scale (Fig. 9c). The driving force for such compression of oxide layer is the considerable increase in molar volume in the process of oxidation: $V_{mol}(Cu) = 7.12$; $V_{mol}(CuO_{0.5}) = 11.7$ and $V_{mol}(CuO) = 12.22 \, cm^3/mol$ [11]. The dense outer layer closes the channels of easy oxygen transfer through the gas phase in porous scale.

At this time, Cu_2O grains appear on the inner surface of scale and soon the cuprite layer expands throughout the larger part of the diffusion zone (Fig. 9d). This may be described as a change in the proportion of CuO to Cu_2O in the two-layered scale as a result of an increasing
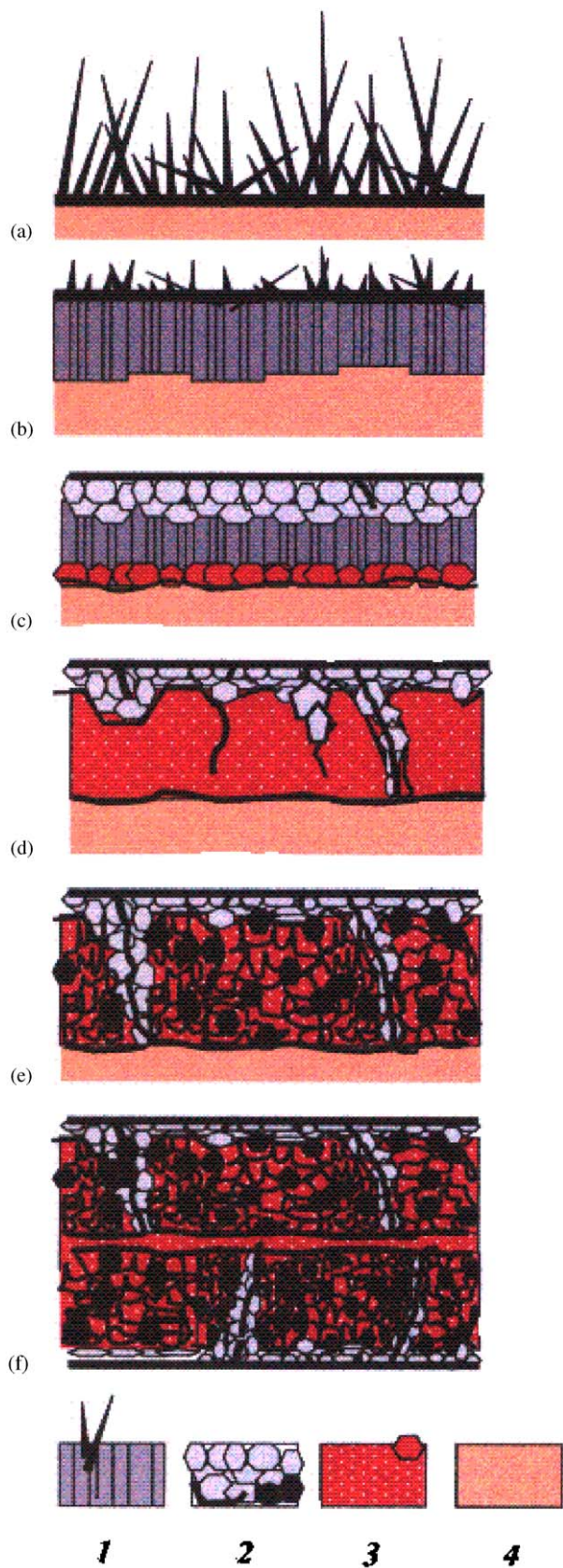
Fig. 9. Schematic presentation of the diffusion zone development: (1) fine-crystalline tenorite; (2) recrystallized tenorite; (3) cuprite; and (4) copper.

diffusion resistance of the outer tenorite layer. The density of diffusion flux through the layer of ith phase in a multilayered diffusion zone may be expressed as [12]:

$$J_i = -D_i \frac{c_i}{RT} \operatorname{grad} \mu_i,$$

where D_i, c_i and μ_i are the diffusion coefficient, molar concentration and chemical potential of the transferred component in the ith layer, respectively; R the gas constant and T the absolute temperature. If D_i and c_i do not change much through the layer and may be estimated by their mean values (which should be the case for copper oxides with not very wide homogeneity regions), that equation is easily integrated and gives for the diffusion in one dimension:

$$J_i = -\bar{D}_i \frac{\bar{c}_i}{RT} \frac{\Delta \mu_i}{\Delta x_i},$$

where Δx_i is the thickness of the ith layer. The difference in the values of chemical potential of the transferred component on the opposite layer boundaries, $\Delta \mu_i$ is entirely determined by the system's thermodynamics and is constant at a specified temperature. For a given reaction rate and so J_i, the quicker is the diffusion transfer and greater D_i in the phase, the wider is the layer of this phase in the diffusion zone.

The same conclusion follows from the equation derived by Valensi [4] for the relation between the molar quantities of oxygen q' and q'' absorbed in two oxide layers and their thicknesses δ' and δ'':

$$\frac{q'}{q''} = \frac{\varphi}{z} \frac{\delta''}{\delta'} \frac{k'}{k''},$$

where k' and k'' are the partial parabolic rate constants for two layers, respectively; φ the ratio of molar volumes of two oxides; and z the coefficient defined by the oxides stoichiometry; for copper oxides $z = 1$. In view of the proportionality of q to δ, the ratio of thicknesses is proportional to the square root from the ratio of partial rate constants.

Therefore, at the initial stages of oxidation, a layer of fine-grained tenorite dominates in the diffusion zone because it allows fast oxygen transfer through its pores and so the effective diffusion coefficient is high. We have not found visible crystalline cuprite grains in the scale at this moment of oxidation. But further growth of densely packed recrystallized tenorite grains increases diffusion resistivity of this layer. That produces a cardinal change in the distribution of oxides in the reaction zone. CuO layer decreases in thickness, instead there arises and grows the layer of another copper oxide—cuprite Cu_2O with higher diffusion permeability. After that, during a long time of further oxidation, the correlation between diffusion resistivities of two oxide phases remains stable as may be judged from the stability of the overall

Table 2
Scheme of the predominant diffusion transfer and reactions on the phase boundaries in the diffusion zone before and after the expansion of Cu_2O layer

Reactions on the phase boundaries before Cu_2O expansion	Scheme of the diffusion transfer	Reactions on the phase boundaries after Cu_2O expansion
$m/2\,O_2 \to m\,O_{(ads)}$, $mCu^{2+} + mO + 2me^- \to mCuO$, $0 \leftrightarrow 2me^- + 2mh^+$, $(m+1)Cu^+ + CuO + (m-1)h^+ \to Cu_2O + mCu^{2+}$ $(m+1)Cu + (m+1)h^+ \to (m+1)Cu^+$	*Air* — CuO — O_2 (through pores) — Cu_2O $\uparrow Cu^+ \downarrow h^+$ — Cu ; CuO Cu^{2+} e^- ; Cu^+ h^+ ; Cu_2O ; Cu	$(n+1)/2\,O_2 \to (n+1)\,O_{(ads)}$, $(n+1)Cu^{2+} + (n+1)O + 2(n+1)e^- \to (n+1)CuO$ $0 \leftrightarrow (2n+2)e^- + (2n+2)h^+$, $(2n+1)Cu^+ + nCuO + h^+ \to nCu_2O + (n+1)Cu^{2+}$ $(2n+1)Cu + (2n+1)h^+ \to (2n+1)Cu^+$
$\mathbf{(m+1)Cu + (m/2)O_2 \to (m-1)CuO + Cu_2O}$	$\mathbf{(m-1) \gg 1}$ $\qquad n > 1$	$\mathbf{(2n+1)Cu + (n+1)/2\,O_2 \to nCu_2O + CuO}$

Cu_2O/CuO compositional ratio in the scale according to XRD data (Figs. 3b and c).

The schemes of diffusion transfer before and after the expansion of cuprite layer are compared in Table 2. The literature data on diffusion coefficients of copper and oxygen in copper oxides and their semiconducting properties [1,2,4,6] were used to deduce which particles are predominantly transferred in each layer and derive the equations of interactions on the phase boundaries in the zone. E.g., copper ions and electron holes were taken as particles dominating in the diffusion transfer through Cu_2O in view of the facts that the diffusion coefficient of copper in cuprite is at least an order of magnitude higher than that of oxygen and Cu_2O is mainly a p-type semiconductor at the studied temperatures [1,2]. The possibility of gas-phase transport of oxygen through porous tenorite layer is also shown in the scheme in Table 2. The assumed predominant transfer of atomic particles, copper ions, outside the specimen agrees with the observations of hollow spaces formed in the center of oxidized specimens (Fig. 8e).

Summary equations of reactions before and after the redistribution of the phases in the diffusion zone are different only in molar ratio of two copper oxides formed as product of the reaction. Subtracting the former from the latter gives the equation of oxidation in the transient period

$$(2n - m)\,Cu + (n - m + 1)/2\,O_2$$
$$\to (n - 1)\,Cu_2O + (2 - m)\,CuO$$
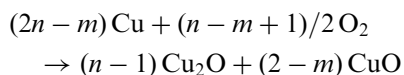
which taking into account a restricted supply of oxygen through a thickened outer layer for a relatively short time of the phase redistribution: $(n - m + 1) \approx 0$, gives

$$(m - 2)\,Cu + (m - 2)\,CuO \to (m - 2)\,Cu_2O.$$
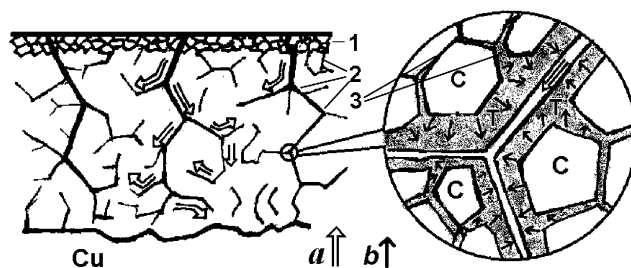
Fig. 10. Diffusion fluxes in fragmented reaction zone: (a) gas-phase diffusion of oxygen and surface diffusion of CuO through cracks; (b) bulk diffusion of copper ions. Phases: (C) cuprite Cu_2O; (T) tenorite CuO (darker areas). (1) Outer CuO layer; (2) macro- and microcracks in product layer; and (3) Cu_2O grain boundaries.

This equation shows that, in this period, the ultimate product of reaction CuO undergoes a reverse transformation: it is reduced to lower copper oxide Cu_2O in the process of continuing oxidation of metal phase.

The most peculiar attribute of further growth of copper scale, as revealed by microscopic studies, is the fragmentation of the diffusion zone: its separation into numerous aggregates of Cu_2O crystals chaotically scattered throughout the zone between thinner layers of CuO grains (Fig. 9e). The scale layers as thin as 40 μm have been observed already fragmented (Fig. 8(g)). Such fragmentation occurs after the formation of the outer dense CuO layer strongly bond to the specimen's surface and the expansion of Cu_2O layer in the zone.

Fragmentation indicates a total rearrangement of the pattern of diffusion fluxes in the reaction zone. Instead of unidirectional (along the plate thickness or the wire radius) diffusion through the oxide layers, the system comes to a very complicated three-dimensional and chaotic pattern of diffusion transfer (Fig. 10).

The model of the layered structure of the diffusion zone used for interpretation of many solid-state reactions is clearly no more applicable for these stages of copper oxidation.

The expansion of cuprite layer in the diffusion zone is perhaps the first step to destroy geometrical regularity of the layers in the diffusion zone. The diffusion permeability of the dense outer CuO layer does not decrease uniformly throughout the entire specimen's surface. There arises some probabilistic distribution of local density and diffusion permeability of recrystallized grains. Consequently, the thickness of the expanding cuprite layer somehow varies along its length (Fig. 9d). This creates preconditions for enclosing Cu_2O blocks with CuO grains.

The crucial role in developing fragmentation belongs, evidently, to macro- and microcracks formed in the scale under mechanical stress arising in crystalline product due to the molar volume increase in the reaction. The volume per one mole of copper increases by 65% in oxidation of Cu to Cu_2O and only 4.3% in further oxidation of Cu_2O to CuO. Cracking creates new channels of fast transfer of oxygen through gas phase and also CuO by surface diffusion. The contribution to this process may be made also by other paths of fast diffusion such as dislocation arrays, etc. that may appear under mechanical stress.

Until metal phase remains in the specimen, the fragmentation of diffusion zone does not result in any unexpected change in oxidation rate. In fact, there are no visible signs that the parabolic kinetics is somehow affected at the period of fragmentation. Apparently, the rate of the reaction is maintained at a high level due to fast oxygen transport to the copper phase boundary through cracks and other channels of fast diffusion. Mechanical stresses on the inner surface of the scale generate microcracks splitting a newly formed coherent oxide layer into separate crystal blocks. Fast supply of oxygen along the boundaries of such blocks produces the layers of CuO crystals around Cu_2O aggregates.

Disappearance of metallic copper in the course of continuing oxidation means the loss of the most powerful source of generating channels of enhanced diffusion. It is at this moment that a rapid decrease in the rate of oxidation is observed.

Therefore, the conclusion on the decisive role of macro- and microcracking in developing the fragmentation of the diffusion zone relies basically on two facts. The first is the geometry of CuO phase distribution that is difficult to relate to something else than the pattern of cracks randomly developed in a crystalline product of reaction. The second fact is that the abrupt deceleration of oxidation occurs just at the time of disappearance of metal phase. It provides evidence that the main source of crack formation lies on the boundary of copper with its oxide layer and is associated with the difference in molar volume between metal and oxide phases.

Until metal phase is not consumed entirely, the growth of the fragmented oxide layer proceeds by means of the transfer through channels of easy diffusion. Although at this stage the kinetics follows the parabolic law, calculated rate constants cannot be associated to the coefficients of lattice diffusion and even to the grain-boundary diffusion in compact blocks of Cu_2O crystals. It is hard to expect any regularity rather than entire chaos in the pattern of macro- and microcracks in a split crystalline layer. Amazingly, the values of parabolic rate constants found for oxidation of different copper specimens and by different authors are in agreement between themselves (Fig. 6) demonstrating quite certain level of reproducibility in diffusion permeability of fragmented copper scale.

Only after complete consumption of metal, the reaction is turning to the rate control by diffusion through the bulk of the compact polycrystalline blocks of Cu_2O and this is the reason of the observed abrupt rate decrease.

In description of solid-state interaction in a multi-phase system the multilayer model of diffusion zone is often used. Its applicability has been many times demonstrated experimentally, especially for compact reagents of regular geometrical form such as plates, spheres or cylinders [4–7]. However, our results show that the multilayer model cannot be used apriori. The real structure of the reaction diffusion zone may appear far more complex than product layers of geometrically regular form.

4. Conclusions

The structure of the diffusion zone undergoes a series of basic rearrangements in the process of deep copper oxidation. They take place against the background of increasing packing density of recrystallizing tenorite CuO grains in oxide layer. Initially, highly permeable fine-grained tenorite layer is formed on the specimen's surface. Then, after the outer dense layer of recrystallized CuO grains develops, the two-layered oxide zone with dominating Cu_2O layer arises. Under mechanical stress due to the difference in molar volume between metal and oxides, a complex pattern of cracks develops in oxide layer providing the channels of fast diffusion transfer. As a result, fragmentation of the diffusion zone occurs—its division into many aggregates of Cu_2O crystals chaotically scattered throughout the zone between thinner layers of CuO grains. A high rate of oxidation is maintained due to plentiful channels of fast diffusion. After complete consumption of metal phase, the creation of new cracks brings to an end and an abrupt decrease in oxidation rate is observed at this moment.

These results show that widely accepted layer model of reaction diffusion zone is far from reality in deep copper oxidation.

References

[1] Yu.D. Tretyakov, The Chemistry of Nonstoichiometric Crystals, Moscow University, Moscow, 1974 (in Russian).

[2] P. Kofstad, Nonstoichiometry, Diffusion and Electrical Conductivity in Binary Metal Oxides, Wiley-Interscience, New York, 1972.

[3] N.P. Lyakishev (Ed.), Diagrams of State of Binary Metallic Systems. V.2, Mashinostroyeniye, Moscow, 1997 (in Russian).

[4] O. Kubaschewski, B.E. Hopkins, Oxidation of Metals and Alloys, Butterworths, London, 1953.

[5] J. Benard (Dir.), Oxydation des metaux. T.2, Gauthier-Villars, Paris, 1964.

[6] K. Hauffe, Reaktionen in und an Festen Stoffen. Bd. 2, Springer, Berlin, 1955.

[7] P. Kofstad, High-Temperature Oxidation of Metals, Wiley, New York, 1966.

[8] V.V. Prisedsky, YU.S. Prilipko, Russ. J. Inorg. Chem. 32 (1987) 2785–2788.

[9] J. Paidassi, J. Acta Met. 6 (1958) 216–220.

[10] V.I. Balakirev, V.F. Barkhatov, Yu.V. Golikov, S.G. Maizel, Manganites: Equilibrium and Unstable States, Russian Academic Science, Ekaterinburg, 2000 (in Russian).

[11] I.L. Knounyants (Ed.), Chemical Encyclopedia. V.2, Sovetskaya encyclopedia, Moscow, 1992, p. 1330–1331 (in Russian).

[12] P.G. Shewmon, Diffusion in Solids, McGraw-Hill, New York, 1965.

[13] Y. Zhu, K. Mimura, M. Isshiki, J. Electrochem. Soc. 151 (2004) B27–B32.